Sustainable Structures
ISSN: 2789-3111 (Print); ISSN: 2789-312X (Online)
http://www.sustain-dpl.com/picnews.asp?id=155
DOI: 10.54113/j.sust.2024.000040

ORIGINAL ARTICLE

Study on the Permeability and Mechanical Properties of Sandy Soil Under Carbon Fiber-Based Urease Mineralization

Zhongping Sun[a], Peng Zhang[a,*], Ben Mou[b,*], Liang Cheng[c]， Shoudong Huo[d] , V.I. Patel[e], Qihang Lv[a]

[a]School of Civil Engineering, Qingdao University of Technology, Qingdao 266033, China.
[b]Department of Civil Engineering, The University of Hong Kong, Hong Kong 999077, China.
[c]School of Environmental and Safety Engineering, Jiangsu University, Zhenjiang 212013, China.
[d]Institute of Geology and Geophysics, Chinese Academy of Sciences, Beijing 100029, China.
[e]Faculty of Building Environment, University of New SouthWales, Sydney, NSW 2052, Australia
*Corresponding Author: Peng Zhang. Email: zhangpchn@qut.edu.cn; Ben Mou, Email: mouben@qut.edu.cn.

Abstract: In recent years, soil solidification by EICP method is a green and environmentally friendly foundation treatment technology that has become popular in the field of geotechnical engineering. Compared with the traditional chemical induction method and the MICP method, the EICP method is not easily restricted by environmental factors associated with engineering geological problems and is green and environmentally friendly with lower cost. In this paper, a study was carried out to improve the seepage-mechanical properties of sandy soils by the EICP method. First, soybean urease solution extraction and its performance optimization methods were explored. Tests were conducted to compare urease extraction and detect activity. The activity of urease was 7.1% higher in deionized water than Laoshan mineral water. Second, the EICP grouting mineralization test was performed by using the carbon fiber reinforcement method. The $CaCO_3$ content, unconfined compressive strength, porosity, permeability and other indicators of the sandy soil were systematically analyzed, and microscopic tests were conducted. The test results showed that after carbon fibers were added to the sand, the mineralization effect of EICP led to the precipitation of $CaCO_3$ that adhered to the surfaces of sand grains and fibers and filled and cemented the pores between sand grains, which improved the integrity of the spatial structure and formed a stable solid sand-fiber monolithic composite structure. When the carbon fiber content was 1.2%, all aspects of performance were optimum. The above test results showed that the carbon fiber-based EICP mineralization method could effectively inhibit the brittle failure and improve the permeability and mechanical properties of sandy soil. This method has good application prospects and development potential for use in engineering geology.

Keywords: Carbon fiber; sandy soil; urease-induced carbonate precipitation; performance optimization; permeability-mechanical properties

1 Introduction

Microbially induced carbonate precipitation (MICP) is a new geotechnical reinforcement

Received: 22 October 2023; Received in revised form: 12 April 2024; Accepted: 18 April 2024

technology that uses microorganisms to induce and regulate the growth of inorganic minerals and improves soil properties by cementing sand particles and filling soil pores [1]. Compared with the traditional chemical induction method, MICP is greener and more friendly to the environment. It has been used successfully in geotechnical engineering The application of MICP technology in geotechnical engineering has many successful cases, and it is widely used in sand consolidation [2-4], restoration of cultural relics [5-7], seepage plugging [8, 9], foundation improvement [10, 11] and other fields. With the continuous promotion and application of MICP, some new problems have emerged in the overall process. For example, the cultivation process of microorganisms is often restricted by the environment, and factors such as temperature [12, 13], humidity [14], and pH [15-17] affect the application of the MICP method. While MICP technology has been fully promoted and applied, some scholars believe that the method has too many requirements for the environment. To ensure that the expected effect can be achieved in the promotion of engineering applications, it is often expensive to create the environment required for cultivating microorganisms. Therefore, new research proposes to obtain urease from crops for urease-induced carbonate precipitation. Gao Y [18] and Nam [19] chose to extract urease from crops and found that the urase improved the effect of inducing mineralization. Pratama [20] chose to extract urease from soybean flour to reduce costs, and through tests such as measurements of urease activity and strength, they found that soybean urease could replace bacteria for soil improvement. Lee [21] found that in terms of inducing carbonate mineralization, the activity of urease extracted from soybean was better than that of urease secreted by microorganisms.

Scholars have recently conducted relevant research on enzyme-induced calcium carbonate precipitation (EICP) in different scenarios. Park [22] used the core plugging test to confirm that the EICP mineralization method caused calcite to precipitate in pores, resulting in a decrease in the permeability of a sandstone core. Gao Y [23] and Almajed [24] conducted field testing and discovered that EICP greatly increased the sandy soils' resistance to wind erosion and surface strength. Chen Y [25] found that the EICP technique could delay the occurrence of capillary barrier breach in sand geotextiles. Moghal [26] found that the $CaCO_3$ precipitate deposited in the soil pores space after EICP treatment could reduce the permeability and swelling of the soil.

The introduction of the fiber reinforcement method effectively improved the mineralization performance of MICP. Mechanical properties such as strength and coefficient of permeability of the soil can be enhanced by adding certain fibers to the soil [27-30], effectively compensating for the brittle defects caused by mineralization of soil [31]. Some scholars combined the soil reinforcement method with the soil mineralization method to explore the influence of the two methods on soil. Qiu [32] found that the doping of carbon fibers promoted the mineralization effect of MICP and resulted in higher strength of the soil. Cheng L [33] conducted an MICP experiment with a mixed source of carbon fiber calcium and magnesium. They found that MICP had good efficiency in improving the thermal conductivity of soil and adding carbon fiber further improved the efficiency.

The traditional chemical grouting mineralization method has side effects on the soil environment. The urease active substance in the MICP grouting mineralization method comes from microorganisms, and the requirements for the test environment and test operation are relatively demanding when cultivating microorganisms. In this study, the EICP grouting mineralization method was tested using sand used sand columns with different carbon fiber contents. The changes in sample permeability and mechanical performance indicators were studied, and a microscopic analysis was conducted to reveal the mechanism of EICP mineralization and interaction. This research method is simple to perform, reduces the requirements for the test environment when cultivating microorganisms and is a more promising method for allowing the surrounding soil to be green and pollution-free. This study provides theoretical support for the extension of the EICP mineralization method to the field of geotechnical engineering.

2 Experimental materials

2.1 Sand and fiber

The tested sand was natural quartz sand (40-60 mesh) from Chuzhou (Anhui Province, China).

Sand grains mainly consisted of SiO_2 (99.64%) and Fe_2O_3 (0.021%). According to GB/T 50123-2019 [34], conducting particle sieving tests to obtain material properties of sand, such as the median particle size (D_{50}), curvature coefficient (C_c) and inhomogeneity coefficient (C_u) (**Fig. 1**). **Table 1** lists the main indicator properties of the tested sand.

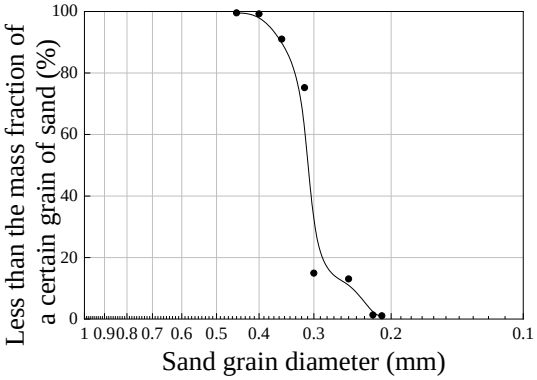

Fig. 1. Sand particle gradation curve.

Table 1. Material properties of sand

Sand sample	D_{50} (mm)	C_c	C_u	G_s	ρ_{max} (g/cm^3)	ρ_{min} (g/cm^3)	e_{max}	e_{min}
Quartz sand	0.307	1.081	1.282	2.653	1.53	1.31	1.023	0.732

Notes: D_{50} is the median particle size, C_c is the curvature coefficient, C_u is the inhomogeneity coefficient, G_s is the the specific gravity, ρ_{max} is the maximum density, ρ_{min} is the minimum density, e_{max} is the maximum porosity, and e_{min} is the minimum porosity.

Carbon fiber can improve the mechanical properties and thermal conductivity of cured sand. It is an ideal reinforcement material. The carbon fiber used in this test was produced by Toray Corporation of Japan (**Fig. 2**). According to GB/T 3362-2017 [35], mechanical properties of carbon fibers obtained from compound filament tensile property tests. **Table 2** lists the main index properties of the carbon fiber.

Fig. 2. Carbon fiber.

Table 2. Material properties of carbon fiber

Diameter (μm)	Length (mm)	Thermal conductivity (W/m·K)	Density (g/cm^3)	Tensile strength (MPa)	Tensile elastic modules (GPa)	Elongation at break (%)	Carbon content (%)
7	6	10	1.76	4900	240	2.0	99%

2.2 Sand column preparation

The sand column samples used in the test were prepared by using a syringe barrel. The operation steps were as follows: 1) Scissors were used to cut a gap from top to bottom of the syringe barrel, it was sealed with glass glue, and penetration-resistant tape was attached. Pad the bottom of the syringe barrel with a strainer to facilitate slurry backflow and avoid leakage of quartz sand. 2) Different ratios

of sand and carbon fiber were prepared; 243.85 g of quartz sand and discrete carbon fibers were weighed corresponding to the mass percentages. The mixture was divided into 5 parts, placed into a beaker, stirred evenly, and placed into a syringe barrel in layers. A metal hammer was used to tamp the mixture (**Fig. 3**) to a predetermined height (22 mm per layer). Control the final height of the sand column specimen at about 110mm, and the density was controlled at 1.46 g/cm^3. According to the different carbon fiber contents, three groups of samples were made for each type.

Fig. 3. Sample compaction.

2.3 Mineralization solution preparation

The activity of urease and the ratio of urease to cementing fluid all affect the formation rate of cementitious materials, the distribution of cementitious materials in the soil. To obtain a better mineralization effect, the chemical cementing solution was configured according to the 1:1 molar concentration of urea and calcium chloride in the solution [36]. First, First, a 1.5 mol/L urea solution was made by combining 45.05 g of urea with 500 mL of distilled water, while a 1.5 mol/L calcium chloride solution was made by combining 83.24 g of anhydrous calcium chloride with 500 mL of distilled water. The two solutions prepared were added to a 1 L Erlenmeyer flask at the same time and vibrated vigorously to ensure that the mixed solution fully reacted to form a chemical cementing solution with a molar concentration of 0.75 mol/L.

3 Experimental design and methods

3.1 Test plan

The soil used in this study was a sandy soil with large pores and good permeability, and infiltration grouting was considered [37, 38]. To evenly distribute the urease-activated polymer gel crystals in the sand column, the two-phase grouting method was performed under a saturated state. That is, in the state of sand column saturation, the chemical cementing fluid and the urease extracting fluid were injected successively. In this study, different proportions of carbon fiber (0%~1.4%, increased by increments of 0.2%) were added to analyze the effect of EICP on sand consolidation. By testing the porosity, permeability, $CaCO_3$ content, and strength of the sample and conducting a microscopic analysis, carried out a study of the permeability mechanical properties of EICP mineralized soils.

3.2 Urease Extraction

During the experiment urease was extracted from soybeans and then treated by filtration, centrifugation, and refiltration. The reaction of urease mineralized alkali to stimulate polymer solution is shown in Eq. (1):

$$C_aCl_2(aq) + CO(NH_2)_2(aq) + 2H_2O(l) \xrightarrow{bacteria} 2NH_4Cl(aq) + CaCO_3(s) \quad (1)$$

In this study, pure very active urease was obtained by using soybeans grown indoors. The steps of the procedure were as follows: 1) The soybeans were ground in batches; a small number of soybeans were put into the electric grinder and ground for 30 seconds into powder (**Fig. 4**a). 2) distilled water was added to the beaker containing soybean flour; the mass ratio of soybean flour and distilled water was 1:5. To make the urease extraction more complete, it was preferable to add water

to the soybean powder. The beaker was placed on a magnetic stirrer (**Fig. 4**b) for uniform, slow, and continuous stirring for 25 min. When the slurry was observed to be evenly stirred, stirring was stopped. 3) The slurry was refrigerated (**Fig. 4**c). The mixed solution separated into two layers of liquid due to gravity, and large insoluble particles of impurities were observed at the bottom of the beaker, which were bean dregs, and the light yellow liquid in the upper layer was urease. 4) The mixed solution was filtered using a 120-mesh screen (**Fig. 4**d**)** to obtain a urease solution without visible impurities. 5) The filtered urease solution was put into a 50 ml centrifuge tube and centrifuge the filtered urease solution at 6000 rpm for 15 minutes to separate the fine insoluble impurities and soluble impurities, which formed insoluble flakes and impurities in water (**Fig. 4**e). 6) Filtration was performed again to obtain a clear urease solution (**Fig. 4**f).

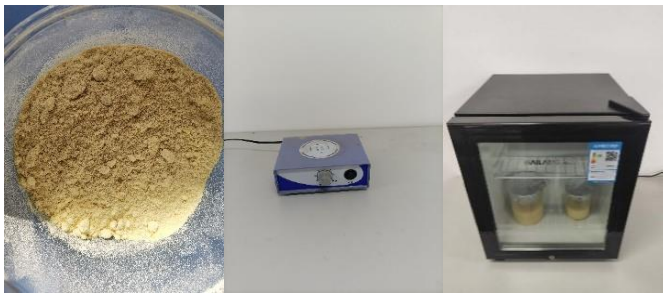

(a) Soy flour (b) Magnetic stirrer (c) Refrigeration

(d) Filter (e) Centrifuge (f) Urease solution

Fig. 4. Test Apparatus.

3.3 Performance optimization of urease

In order to have better results in the grouting mineralization test, the performance of urease solution is a crucial factor that needs to be tested for its activity. The following reaction occurs (Eq. (2)) when the urease solution is added to the urea solution. This reaction gradually produces charged particles in a solution that was originally free of charged ions, thereby enhancing the conductivity of the solution. Therefore, the higher the activity of the urease solution, the faster the rate of urea hydrolysis and the faster the conductivity of the solution is enhanced. Urease activity can be characterized by means of a thermal conductivity meter.

$$CO(NH_2)_2(aq) + 2H_2O(l) \xrightarrow{bacteria} 2NH_4^+(aq) + CO_3^{2-}(aq) \quad (2)$$

The specific test of urease activity detection was as follows: When detecting activity, it is advisable to apply 1 mL of urease extract to 10 mL of urea solution with a concentration of 1.5 mol/L. In the course of the test, we performed a number of tests in order to measure quantities conveniently with precise proportions. First, the test tube was filled with 5 mL of urea solution, which had a concentration of 3 mol/L. Then 4 mL of water and 1 mL of urease extract were added into the test tube, and the test tube was shaken quickly and completely. Following the insertion of the conductivity meter's probe into the mixture, the number on the display of the conductivity meter increased rapidly from 0, and after a period of high-speed growth, the growth rate became increasingly slower. When it reached 2 ms/mL, the stopwatch was turned on, and this time was marked as 0 min. After 1 min, the readings of the conductivity meter were recorded and then recorded at 2 min, 3 min, 4 min, and 5 min in turn. Starting the timer from the moment when the instrument reached 2 ms/mL could effectively reduce the measurement error.

To release the maximum activity of urease in the solution, a control test was set up for the water quality used in this activity test. When the room temperature was 22 ℃, the measured conductivity value represented the test data of urease solution activity (**Fig. 5**).

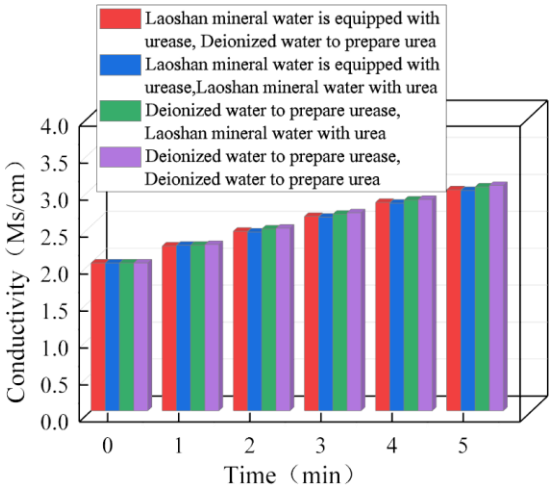

Fig. 5. Urease solution activity expression based on electrical conductivity.

The measurement method of the conductivity meter: Referring to the method introduced by Whiffin [39], the value calculated according to Eq. (3) characterized the activity of urease solution.

$$a = \Delta E / \Delta t \times 11.11 \times d \tag{3}$$

where a is the characteristic value of urease extract activity, ΔE is the conductivity difference of the solution to be tested in a certain time interval, Δt is the interval time, and d is the dilution ratio of the urease extract.

According to the above calculation method, the activities of the four groups of urease solutions were obtained (**Table 3**). The unit U in the table represents the decomposition of 1 mol of urea per minute.

Table 3. Characteristic values of urease activity in each test group

Test group	Urease activity (U/mL)
Laoshan mineral water used to extract urease, Deionized water used to prepare urea	22.00
Laoshan mineral water used to extract urease, Laoshan mineral water mixed with urea	21.78
Deionized water used to prepare urease, Laoshan mineral water mixed with urea	22.89
Deionized water used to prepare urease, Deionized water used to prepare urea	23.33

Table 3 shows that when the urease solution and urea detection solution were prepared with deionized water, the activity of urease reached 23.33 U/mL, which was 7.1% higher than that of the urease solution extracted entirely from Laoshan mineral water.

3.4 Urease-induced carbonate precipitation grouting mineralization

The EICP grouting mineralized sand test device included a U-shaped tube, syringe tube, peristaltic pump, waste liquid treatment tank, urease solution, cementing liquid, and fixtures. The fixing device was a test bench made in this laboratory, and the syringe tube with the sand column could be placed in the small hole of the test bench to facilitate the connection of the syringe tube with the U-shaped tube and the peristaltic pump. The steps of EICP grouting mineralized sand were as follows: 1) The bottom of the syringe tube was first connected to the U-shaped tube, and the top of the tube is then connected to the peristaltic pump. A peristaltic pump was used to inject 1.4 times the pores at a rate of 5 mL/min using the upward flow method. volume of deionized water, when the

liquid level in the syringe was slightly higher than the sand surface, the sand column was in a saturated state. 2) The two-phase injection method was used for EICP treatment. First, 74 mL of urease extract was poured into the top of the syringe. Referring to the bacterial liquid injection method proposed by Cui Mingjuan, a peristaltic pump was used at a rate of 5 mL/min. It was injected into the specimen and allowed to stand for 2 hours to make the urease fully adhere to the soil particles. Then, 74 mL of cementing solution was injected, and when the chemical cementing solution disappeared on the sand surface, the self-priming peristaltic pump was immediately turned off. 3) After the sample was left to stand for 24 hours, step 2 was repeated for a total of 7 days of grouting to obtain the EICP treatment and solidification of the molded sand column. The EICP treatment process device used in this experiment is shown in **Fig. 6**a, b.

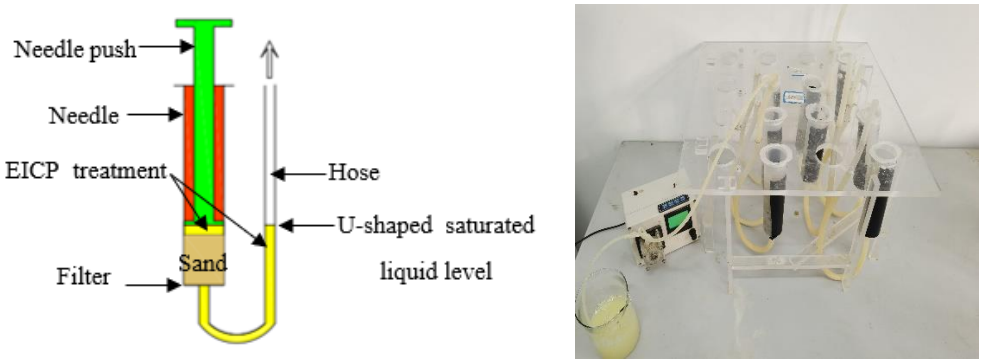

(a) EICP Downflow Injection Processing (b) Saturated sample with water

Fig. 6. EICP grouting mineralization.

4 Test method

4.1 $CaCO_3$ content test

The content of $CaCO_3$ was tested by the pickling method [40]. Its specific operation was as follows: (1) A small sample was weighted, its mass was recorded as m_1, and then the test piece was crushed. (2) A beaker containing a crushed test block was filled with an excess of 1 mol/L hydrochloric acid to initiate a reaction. The calcium carbonate in the test piece reacted completely with hydrochloric acid. The remaining solid matter in the beaker was cleaned and dried completely, and the mass was recorded as m_2.

$$\omega(\%) = \frac{m_1 - m_2}{m_1} \tag{4}$$

4.2 Unconfined compressive strength test

(a) Compression failure of the sample (b) The cracked sample (c) Failure surface of the sample

Fig. 7. strength test.

The test soil in this study was sand treated with carbon fiber-doped EICP mineralization, and the effects of EICP mineralization and carbon fiber reinforcement on the strength of the soil were explored. The instrument used in the test was a strain gauge unconfined compressive strength tester.

First, the prepared specimen was placed on the instrument, the height of the bottom was adjusted so that the specimen was just in contact with the upper pressing piece, and then the force gauge was adjusted so that the reading at this moment was 0 mm. After the above preparations were performed, the pressure was slowly increased to measure strength of the specimen (**Fig. 7**).

4.3 Porosity test

The drying method was used in this test to measure the specimen's volume change [41]. First, after injecting water into the hardened sand to make it saturated, the specimen was allowed to stand for eight hours before the wet weight (m_ω) was measured. Then, the saturated specimen was placed into the oven to dry to constant weight, and the specimen's dry weight (m_d) was determined. The mass of water contained in the pores of the specimen is obtained by calculating the mass variation between the initial and subsequent specimens, and the porosity n of each sand column was calculated by Eq. (5).

$$n = \frac{m_\omega - m_d}{\rho_\omega V} \tag{5}$$

4.4 Penetration test

The sandy soil in this study had pores, and liquids such as groundwater could flow from the pores to form seepage forces, which could remove mineralized crystals or soil particles, disrupt the soil's structure, which will subsequently have an impact on the soil's mechanical characteristics. The indoor penetration test was divided into the constant head method and the variable head method in principle. The sand used in this test was relatively fine, and thus the variable head method was used. The operation steps were as follows: First, the sand column after grouting was placed on a homemade bench, water was poured at the top, and when there were stable water droplets at the bottom, then connect the spout at the lower end of the syringe with the head gauge tube filled with water to saturate the sand column and form an initial head difference. Then, the head valve was opened, and the measurement was started. The measuring device is shown in **Fig. 8**a, and the schematic diagram is shown in **Fig. 8**b. Referring to geotechnical test method standards [34], the permeability coefficient was calculated using Eq. (6).

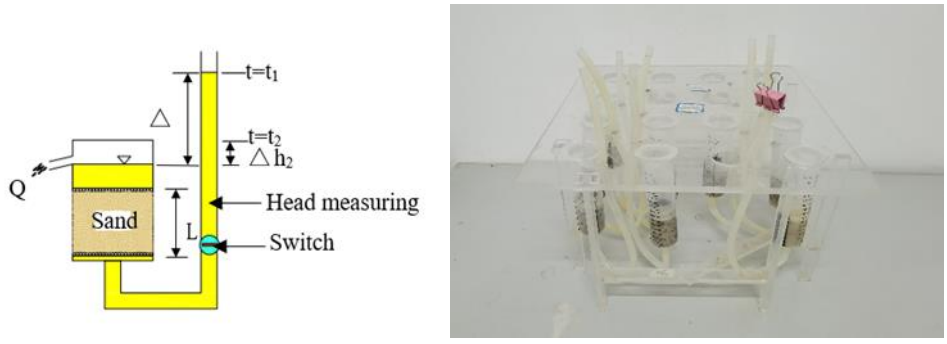

(a) Schematic diagram of the penetration test (b) Penetration test device

Fig. 8. Penetration test.

$$k = 2.3\frac{aL}{A(t_2 - t_1)} Lg\frac{\Delta h_1}{\Delta h_2} \tag{6}$$

where L is the seepage diameter, equal to the height of sand column specimen, t_1 is the starting time, t_2 is a certain time after starting, Δh_1 is the initial head difference, and Δh_2 is the head difference at time t_2.

4.5 Microscopic testing

Scanning electron microscopy (SEM) was used in this study. A desktop scanning electron microscope with a built-in energy spectrometer produced by Hitachi, Japan was used. It could not

only observe the microscopic morphology of the material surface but also conduct qualitative analysis on the composition of a small area on the material surface at the same time. After the strength test, undoped cement block samples (no carbon fiber) samples doped with carbon fiber (1.2% and 1.4%) were selected, and typical parts with relatively flat cross sections were tested with the electron microscope. Then, gold spraying treatment was carried out under vacuum to maximize the reduction in the charge generated by the electron beam. Finally, the test block was magnified 1000 times for electron microscope scanning.

5 Results and Analysis

5.1 Analysis of $CaCO_3$ content results

By analyzing the relationship between different carbon fiber dosage and the change of calcium carbonate content in the sand column (**Fig. 9**), showed that with the increase of carbon fiber dosage, the $CaCO_3$ content shows a tendency of increasing and then decreasing. The $CaCO_3$ content rose by 45.1% when the carbon fiber percentage increased from 0% to 0.6%. When the carbon fiber content was increased from 0.8% to 1.2%, it only increased by 30.13%, at which point the $CaCO_3$ content peaked. The production of $CaCO_3$ fell by 5.9% as the carbon fiber content rose to 1.4%. Therefore, there was not a direct linear relationship between the amount of $CaCO_3$ produced and the amount of carbon fiber added, which was related to the interaction between urease, cementing fluid, carbon fiber and soil. When the amount of carbon fiber was less, it occupied less sand pore space, and there is more space in the sand body for urease to adsorb and participate in the EICP process, and the $CaCO_3$ precipitated by a series of reactions. When the quantity of carbon fiber doping reaches a certain degree, the carbon fibers contact each other to form a spatial network that affects the normal infiltration and migration of urease in the sample, and the hydrolysis rate of urea began to slow, but the $CaCO_3$ precipitation still slowly increased. When the dosage exceeded 1.2%, the carbon fiber occupied a large quantity of pore space. The limited pore space inhibited the metabolic activity of urease, the production of $CaCO_3$ was impacted, and prevented the cementing fluid from penetrating into the sand for the EICP process. Therefore, the formation of $CaCO_3$ was slightly less than before.

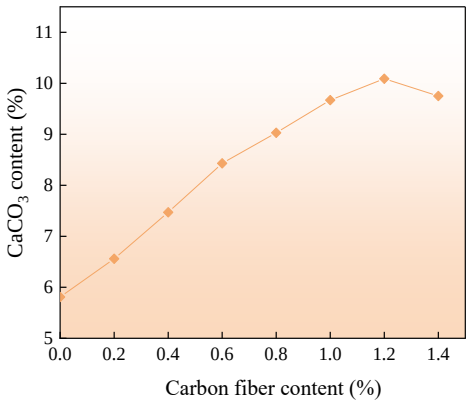

Fig. 9. Variation of $CaCO_3$ content in the sand column.

5.2 Unconfined compressive strength test results

The analysis of the results of sand column strength (**Fig. 10**) shows that as carbon fiber dosage is increased, the unconfined compressive strength typically rises before falling. Due to the cementing effect of calcium carbonate deposited between carbon fibers and sand particles. The carbon fiber and sand solidified together, and carbon fibers were anchored in the sand, which made the carbon fiber's surface rougher and expanded its area in contact with the sand, thereby increasing the friction between the carbon fiber and the sand. The interaction between the two enhanced the interfacial force between the carbon fiber and calcium carbonate, thereby increasing the overall compressive performance of the sand specimen. When the fiber content was low (0.2%~0.6%), the amount of $CaCO_3$ significantly increased, and the interfacial force between the carbon fiber and $CaCO_3$ also increased. However, it was difficult to form an effective fiber network structure due to the large spacing of the spatial

distribution of fibers. With increasing fiber content (0.6%~0.12%), the growth rate of $CaCO_3$ production slowed. But, the overall increase in compressive strength has improved considerably. But the increase in the overall compressive strength greatly improved. This was due to the interfacial force between the $CaCO_3$ reinforced fiber and the sand, and the spatial distribution of carbon fiber transformed into a three-dimensional network structure, which exerted a three-dimensional reinforcement effect of carbon fiber and increased the integrity and stability of the specimen. Once carbon fiber doping hits a certain threshold (the amount of carbon fiber was 1.2%), the $CaCO_3$ precipitation reached the peak, all of them were evenly attached to the carbon fiber, and the integrity of the spatial structure reached the optimal state. As the fiber content continued to increase (1.4%), the surface area of the carbon fiber increased. However, the specimen's unequal attachment to the carbon fiber resulted from a decrease in $CaCO_3$ synthesis, and weakened interfacial forces between fibers and sandy soil. Cause stress concentration phenomenon, reduce the integrity and compressive strength of the specimen.

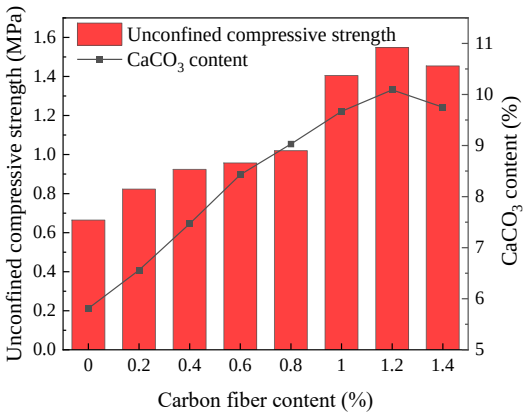

Fig. 10. Unconfined compressive strength of the sand column.

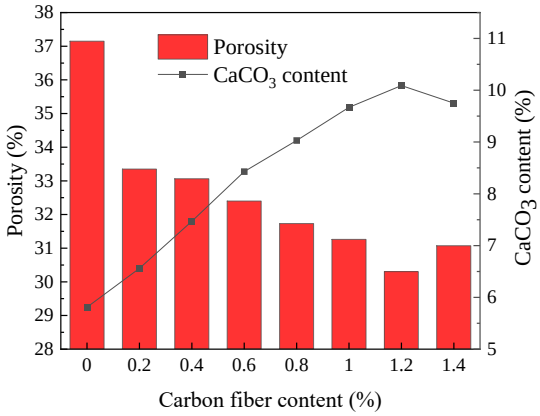

Fig. 11. Sand column porosity.

5.3 Analysis of porosity test results

By analyzing the porosity of EICP-treated sand columns with varying carbon fiber dosage (**Fig. 11**) showed that for pure sand columns (carbon fiber content 0%), under the action of EICP, the porosity was 37.15%. The porosity before mineralized grouting was 44%, which was reduced by 6.85%. It can be seen that the EICP mineralization grouting method had a significant effect on increasing the compactness and reducing the porosity of the soil. At the same time, its porosity was significantly impacted by the carbon fiber content of the specimens. When the sand column's carbon fiber content was low, by increasing the amount, its filling ratio in the pores could be increased. Besides the adsorption area of $CaCO_3$ precipitated by urea hydrolysis on the carbon fiber could be increased during the EICP process. At this moment, the spatial distribution of carbon fibers gradually became a three-dimensional spatial network structure. $CaCO_3$ binds the separated sand grains together and binds evenly to the carbon fibers. It compacts the sample's pores and limits the movement and distortion of the sand grains. The combined effect of the porosity decreased continuously with increasing carbon fiber content. But once carbon fiber doping hits a certain threshold (the amount of carbon fiber was 1.2%), the pore space structure of the sand column was the most compact, and the porosity reached the minimum. Continuing to add its dosage, at this time, the carbon fiber occupied a certain pore space. The limited pore space affected the activity of urease and prevented the cementing fluid from penetrating into the sand, thereby affecting the quantity of $CaCO_3$ precipitation and the reduction of the adsorption area on the carbon fiber during the entire EICP process. As a result, the pore volume of the sand column increased.

5.4 Analysis of permeability test results

The undisturbed sand column's permeability coefficient was 2.08×10^{-3} cm/s, and the sand column after one cycle of EICP mineralization had a permeability coefficient of 4.76×10^{-5} cm/s. It

was magnitude lower of penetration rates. According to the analysis of permeability coefficients of EICP-treated sand columns with different carbon fiber dosages (**Fig. 12**), under the joint action of EICP mineralization and carbon fiber on the specimens, with the increasing quantity of carbon fiber in the specimens, the amount of $CaCO_3$ precipitated by the reaction increased, and the pore space inside the specimens was blocked by the precipitated calcium carbonate, resulting in a certain degree of decrease in the permeability of the specimens. The permeability reached its lowest value when the carbon fiber doping reached 1.2%, with a permeability coefficient of 1.92×10^{-5} cm/s. When the carbon fiber doping was increased from 1.2% to 1.4%, the permeability coefficient of the specimens instead increased to 2.26×10^{-5} cm/s. At this time, with the increase of carbon fiber doping, the specimens is occupied by carbon fibers to increase the pore space of the specimens. But due to the reduction in the internal pore space, the urease activity decreased, and the cementing fluid had more difficulty penetrating into the specimens. In turn, it affected the amount of $CaCO_3$ precipitated by the hydrolysis of urea, the area attached to the carbon fiber decreased, and the clogged area of pore space increased, leading to an increase in the sand column's permeability coefficient.

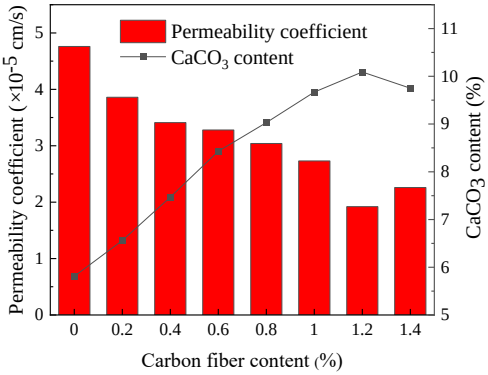

Fig. 12. Sand column permeability coefficient value.

5.5 Microscopic test results

Fig. 13 shows the SEM images of the cured specimens without carbon fiber and with carbon fiber contents of 1.2% and 1.4%. From the 1000 times magnified SEM image (**Fig. 13**a) of the cured sample without carbon fiber content, the calcium carbonate precipitate generated by EICP adheres to the sand grains and fills the pores to some extent. When the grout was completely saturated, it filled the pore space and formed calcium carbonate crystals that were deposited in the pore space. It were wrapped by precipitated $CaCO_3$ crystals of the sand grains, which improved the integrity of the structure, thereby strengthening the sand samples that were treated with EICP.

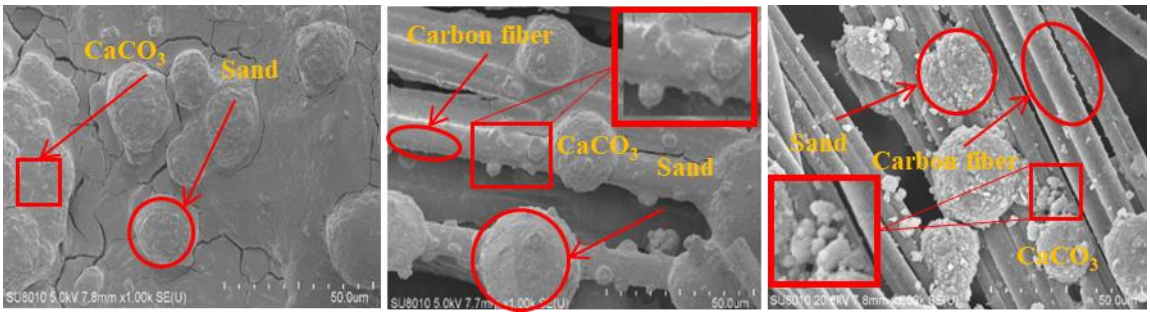

(a) Undoped carbon fiber (b) Carbon fiber content 1.2% (c) Carbon fiber content 1.4%

Fig. 13. SEM image of the carbon fiber-doped sample.

The cured sample (**Fig. 13**b), which had a 1.2% carbon fiber content, was examined under a 1000 times magnified SEM image to reveal the fibers pass through the holes between the sand grains to form a three-dimensional mesh structure. In some measure, this structure limited the movement and deformation between the sand grains. When the shear failure surface appeared on the sample, the fibers on the shear surface generated tensile stress. It made up for the strength loss caused by the

destruction of the nearby soil and could also inhibit the further occurrence of the shear plane. A this point in time, a lot of $CaCO_3$ precipitate was attached to the surfaces of the carbon fibers, the contact between the carbon fiber and the sand, and the surface of the sand. This increased the amount of $CaCO_3$ produced. Carbon fiber played the role of a bridge in the EICP process, while calcium carbonate bonded the spaced sand particles together and evenly attached to the carbon fiber to play a bonding role. The integrity of the spatial structure reached the optimal state. And the quantity of carbon fiber rose (reaching a certain amount), the bridging effect became more obvious, and more calcium carbonate precipitates were formed by the solidified body, thus forming a stable solid sand-fiber overall composite structure. The surface roughness of the carbon fiber increased, thereby raises the specimen's internal friction, which raises strength of the specimen.

When carbon fiber doping is increased to a certain level after (**Fig. 13**c**)**, the carbon fibers with a content of 1.4% were entangled. Occupying a certain pore space inside the sand column, the limited pore space affected the activity of urease and prevented the cementing fluid from penetrating into the sand. At this time, $CaCO_3$ crystals precipitated only on the surfaces of the fibers， thereby this results in lower $CaCO_3$ production. The specific surface area of the carbon fiber increases, the production of $CaCO_3$ decreases and unevenly wrapped around the carbon fiber, part of the calcium carbonate is easily damaged by the rupture phenomenon. The interfacial forces between fibers and sand weakened, resulting in stress concentrations and thereby reducing the integrity and compressive strength of the sample.

6 Conclusions

In this study, a series of experimental studies were carried out on urease, which could induce calcium carbonate cementation. Orthogonal experiments were conducted on sand columns by using EICP grouting mineralization and adding carbon fiber. In this experiment, multiple control groups were set up to highlight the effects of the EICP grouting mineralization treatment and carbon fiber on the performance of the sand columns. By carrying out the mineralization test of sand column EICP grouting with different carbon fiber dosage, the changes in the indexes such as porosity, permeability coefficient, $CaCO_3$ content, and unconfined compressive strength of the study specimens were compared and analyzed. The results showed the following:

(1) Under the same conditions, using deionized water instead of Laoshan mineral water to dissolve soybean powder and extract urease increased the activity of the urease solution by 7.1%.

(2) Since calcium carbonate deposited between the carbon fibers and sand particles has a cementation effect, the carbon fiber and the sand solidified together, and the carbon fibers were anchored in the sand, increasing the roughness of the carbon fiber surfaces and the contact areas with the sand, thereby increasing the friction between the carbon fibers and sand, and the interaction between the two enhanced the interfacial force between them. Therefore, the overall compressive performance of the sand specimen increased. As the content of carbon fiber increased, the $CaCO_3$ content and unconfined compressive strength also increased. The dosage reached a peak at 1.2%, and the $CaCO_3$ content decreased when the dosage exceeded this point.

(3) The EICP grouting mineralization method increased the compactness of the soil and significantly reduced the porosity. Under the action of EICP grouting, mineralization decreased the porosity by 6.85%. Moreover, with the increasing amount of carbon fiber in the specimen, the quantity of $CaCO_3$ precipitated by the reaction increased, and it blocked the pore space inside the specimen. As a result, the permeability of the specimen decreased to a certain extent. Under the action of EICP and the optimal amount of carbon fiber (1.2%), the pore space structure of the specimen was the most compact, the porosity reached the minimum, and the permeability reached the lowest value.

(4) Carbon fibers acted as a bridge during the EICP process, while calcium carbonate acted as a bond, binding the sand grains together to form a stable solid sand-fiber monolithic composite structure. The surface of the carbon fiber is coated with $CaCO_3$ that is deposited during the EICP process, which increased the internal friction of the specimen and improved the strength of the specimen. However, when the amount of carbon fiber was increased to a certain extent, the carbon fibers did not entangle, affecting the precipitation of $CaCO_3$ crystals only on the fiber surface. In addition, some calcium

carbonate was easily damaged and cracked, and the interfacial force between the fiber and sand weakened, resulting in stress concentrations that affected the performance of the sample.

(5) In the process of this study, the solidification of quartz sand material was studied, and good results were obtained. However, the reinforcement materials studied individually. EICP can be applied to the reinforcement of various sands and soils in future research and has good application prospects and development potential for use in engineering geology.

Acknowledgement

The authors would like to acknowledge financial support from the national key research program of China(2022YFB3904600), the National Natural Science Foundation of China (Grant No: 42177167), the Natural Science Foundation of Shandong Province (ZR2019QEE008).

CRediT authorship contribution statement

Zhongping Sun: Writing – original draft, Formal analysis. **Peng Zhang**: Supervision, Funding acquisition. **Ben Mou**: Supervision, Funding acquisition. **Liang Cheng**: Supervision, Funding acquisition. **Shoudong Huo**: Supervision, Funding acquisition. **Qihang Lv**: Data curation, Formal analysis.

Conflicts of Interest

The authors declare that they have no known competing financial interests or personal relationships that could have appeared to influence the work reported in this paper.

References

[1] Liu HL, Ma GL, Zhao C, et al. Macro-micro-mechanical mechanism of calcareous sand reinforced by micro organisms. Journal of Civil and Environmental Engineering (Chinese and English) 2020; 42(4): 205-206. https://doi.org/10.11835/j.issn.2096-6717.2020.097.

[2] Rizvi ZH, Nikolić M, Wuttke F. Lattice element method for simulations of failure in bio-cemented sands. Granular Matter 2019; 21(2):1-14. https://doi.org/10.1007/s10035-019-0878-6.

[3] Duo L, Kan L T, Hui LZ, et al. Experimental investigation of solidifying desert aeolian sand using microbially induced calcite precipitation. Construction and Building Materials 2018; 172: 251-262. https://doi.org/10.1016/j.conbuildmat.2018.03.255.

[4] Wang X, Li C, He J. A highly effective strain screened from soil and applied in cementing fine sand based on MICP-bonding technology. Journal of biotechnology 2022; 350: 55-66.https://doi.org/10.1016/j.jbiotec.2022.03.016.

[5] Liu SY, Yu J, Zeng WL, Peng XQ, Cai YY, Tu BX. Study on the effect of microbe-induced calcium carbonate precipitation in repairing cracks in triadic soil. Journal of Rock Mechanics and Engineering 2020; 42(4): 205-206. https://doi.org/10.11835/j.issn.2096-6717.2020.097.

[6] He Jh. Experimental research on the repair of fractured white marble stone by MICP. Tsinghua University 2019. https://doi.org/10.27266/d.cnki.gqhau.2019.000485.

[7] Huang XS. Experimental research on repairing cracks in masonry ancient buildings based on induced calcium carbonate precipitation technology. Henan University 2021. https://doi.org/10.27114/d.cnki.ghnau.2021.000494.

[8] Cuthbert MO, McMillan LA, Handley SS, et al. A field and modeling study of fractured rock permeability reduction using microbially induced calcite precipitation. Environmental science & technology 2013; 47(23):13637-13643. https://doi.org/10.1021/es402601g.

[9] Gao Y, Tang X, Chu J, et al. Microbially induced calcite precipitation for seepage control in sandy soil. Geomicrobiology Journal 2019; 36(4): 366-375. https://doi.org/10.1080/01490451.2018.1556750.

[10] Gomez MG, Martinez BC, DeJong JT, et al. Field-scale bio-cementation tests to improve sands. Proceedings of the Institution of Civil Engineers-Ground Improvement 2015; 168(3): 206-216. http://dx.doi.org/10.1680/grim.13.00052.

[11] Saneiyan S, Ntarlagiannis D, Ohan J, et al. Induced polarization as a monitoring tool for in-situ microbial induced carbonate precipitation (MICP) processes. Ecological engineering 2019; 127: 36-47. https://doi.org/10.1016/j.ecoleng.2018.11.010.

[12] Gillman E, Morgan MA, Sherwood M. Urease activity in Irish soils at 6 C. Royal Irish Academy 1995; 19-26. https://www.jstor.org/stable/20504489.

[13] Ahenkorah I, Rahman MM, Karim MR, et al. Unconfined compressive strength of MICP and EICP treated sands subjected to cycles of wetting-drying,freezing-thawing and elevated temperature: Experimental and EPR modelling. Journal of Rock Mechanics and Geotechnical Engineering 2022; https://doi.org/10.1016/j.jrmge.2022.08.007.
[14] Li Jie, Fang XW, Shen CN, etc. Research on the Effect of Moisture Content on the Mechanical Properties of Coral Sand Microbial Solidification. Industrial Building 2016; 46: 93-97. https://doi.org/10.13204/jgyjz201612019.
[15] Stocks FS, Galinat JK, Bang SS. Microbiological precipitation of CaCO3. Soil Biology and Biochemist-ry 1999; 31(11): 1563-1571. https://doi.org/10.1016/S0038-0717(99)00082-6.
[16] Lai Y, Yu J, Liu S, et al. Experimental study to improve the mechanical properties of iron tailin-gs sand by using MICP at low pH. Construction and Building Materials 2021; 273: 121729. https://doi.org/10.1016/j.conbuildmat.2020.121729.
[17] Yin LY, Tang CS, Xie YH, Lu Chao, Jiang NJ, Shi Bin. Factors affecting the performance of rock and soil materials by microbial mineralization. Rock and Soil Mechanics 2019; 40(07): 2525-2546. https://doi.org/10.16285/j.rsm.2018.0520.
[18] Gao Y, He J, Tang X, et al. Calcium carbonate precipitation catalyzed by soybean urease as an improvement method for fine-grained soil. Soils and Foundations 2019; 59(5): 1631-1637. https://doi.org/10.1016/j.sandf.2019.03.014.
[19] Nam IH, Chon CM, Jung KY, et al. Calcite precipitation by ureolytic plant (Canavalia ensifor-mis) extracts as effective biomaterials. KSCE Journal of Civil Engineering 2015; 19(6): 1620-1625.https://doi.org/10.1007/s12205-014-0558-3.
[20] Pratama GBS, Yasuhara H, Kinoshita N, et al. Application of soybean powder as urease enzyme replacement on EICP method for soil improvement technique. IOP Publishing, 2021, 622(1): 012035. https://doi.org/10.1088/1755-1315/622/1/012035.
[21] Lee S, Kim J. An experimental study on enzymatic-induced carbonate precipitation using yellow soybeans for soil stabilization. KSCE Journal of Civil Engineering 2020; 24(7): 2026-2037. https://doi.org/10.1007/s12205-020-1659-9.
[22] Park J, Choi BY. Feasibility study of enzyme-induced calcium carbonate precipitation (EICP) for CO2 leakage prevention. Geosciences Journal 2022; 26(2): 279-288. https://doi.org/10.1007/s12303-021-0033-3.
[23] Gao YF, Meng H, He J, Qi YS, Hang L. Field test of crude soybean urease-induced calcium carbonate deposition to inhibit wind erosion of wind-sand soil. Journal of Central South University 2020; 27(11): 3320-3333. https://doi.org/10.1007/s11771-020-4549-x.
[24] Almajed A, Lemboye K, Arab MG, et al. Mitigating wind erosion of sand using biopolymer-assisted EICP technique. Soils and Foundations 2020; 60(2): 356-371. https://doi.org/10.1016/j.sandf.2020.02.011.
[25] Chen Y, Gao Y, Guo H. Bio-improved hydraulic properties of sand treated by soybean urease induced carbonate precipitation and its application Part 2: Sand-geotextile capillary barrier effect. Transportation Geotechnics 2021; 27: 100484. https://doi.org/10.1016/j.trgeo.2020.100484.
[26] Moghal AA B, Lateef MA, Abu SMS, et al. Heavy metal immobilization studies and enhancement in geotechnical properties of cohesive soils by EICP technique. Applied Sciences 2020; 10(21): 7568. https://doi.org/10.3390/app10217568.
[27] Pan JX. Research on mechanical properties of fiber blended reinforced soil. Southwest University 2020. https://doi.org/10.27684/d.cnki.gxndx.2020.003291.
[28] Liang JL, Zhao JL, Yuan J, Qiu RK, et al. Mechanical properties and particle shape analysis of carbon fiber microbial solidified sand. Science Technology and Engineering 2022; 22(30):13434-13440. https://doi.org/10.3969/j.issn.1671-1815.2022.30.036.
[29] Zhang HD, Li HF, Li HY, Liu J, Hu TJ, Zhang HP, Zhao NN, et al. Experi-mental research on strength characteristics of palm fiber reinforced soil. Mineral Exploration 2021; 12(05): 1264-1271. https://doi.org/10.3969/j.issn.1674-7801.2021.05.020.
[30] Xiao ZY. Experimental research on soil reinforcement based on improved microbial-induced calcium carbonate deposition technology. North China University of Water Resources and Electric Power 2021. https://doi.org/10.27144/d.cnki.ghbsc.2021.000121.
[31] Shao W, Cetin B, Li Y, et al. Experimental investigation of mechanical properties of sands reinforced with discrete randomly distributed fiber. Geotechnical and Geological Engineering 2014; 32(4): 901-910. https://doi.org/10.1007/s10706-014-9766-3.
[32] Qiu R, Tong H, Fang X, et al. Analysis of strength characteristics of carbon fiber–reinforced micr-obial solidified sand. Advances in Mechanical Engineering 2019; 11(11): 1687814019884420. https://doi.org/10.1177/1687814019884420.
[33] Cheng L, Afur N, Shahin MA. Bio-Cementation for improving soil thermal conductivity. Sustainability 2021; 13(18): 10238. https://doi.org/10.3390/su131810238.

[34] GB/T 50123—2019. Standards for geotechnical test methods. China Planning Press 2019. https://slt.henan.gov.cn/2021/04-12/2124270.html.
[35] GB/T 3362—2017. Test method for tensile properties of carbon fiber multifilament. Standard Press of Chin a 2017. https://openstd.samr.gov.cn/bzgk/gb/newGbInfo?hcno=54B16FC0761DAFF523E8E5290B61555B.
[36] Carmona JPSF, Venda Oliveira PJ, Lemos LJL, et al. Improvement of a sandy soil by enzymatic calcium ca rbonate precipitation. Proceedings of the Institution of Civil Engineers-Geotechnical Engineering 2018; 17 1(1): 3-15. https://doi.org/10.1680/jgeen.16.00138.
[37] Wu LY, Miao LC, Sun XH, Chen RF, Wang CC. Experimental study on the stabilization of sandy soil indu ced by plant-derived urease with calcium carbonate. Journal of Geotechnical Engineering,2020,45(04):714 -720. https://doi.org/10.11779/CJGE202004014.
[38] Almajed A, Abbas H, Arab M, et al. Enzyme-Induced Carbonate Precipitation (EICP)-Based methods for ec ofriendly stabilization of different types of natural sands. Journal of Cleaner Production 2020; 274: 122627. https://doi.org/10.1016/j.jclepro.2020.122627.
[39] Whiffin VS,Van Paassen LA, Harkes MP. Microbial carbonate precipitation as a soil improvement techniqu e .Geomicrobiology Journal 2007; 24: 417-423. https://doi.org/10.1080/01490450701436505.
[40] Ma GL, He X, Lu HM, Wu HR, Liu HL, Chu J, Xiao Y. Strength of coarse sand solidified by nucleating mi croorganisms loaded with kaolin particles. Acta Geotechnical Engineering 2021; 43(02): 290-299. https://d oi.org/10.11779/CJGE202102009.
[41] Luo XW. Experimental Research on Sand Solidification Based on Microbe-Induced Calcium Carbonate Pr ecipitation Technology (MICP). Nanjing University 2018. https://doi.org/10.27235/d.cnki.gnjiu.2018.0003 91.